

Role of the Spacer Stereochemistry on the Structure of Solid-Supported Gemini Surfactants Aggregates

Giulio Caracciolo,[†] Daniela Pozzi,[†] Giovanna Mancini,[‡] and Ruggero Caminiti^{*†}

Department of Chemistry, University of Rome "La Sapienza", P.le A. Moro 5, 00185 Rome, Italy, and IMC-CNR c/o Department of Chemistry, University of Rome "La Sapienza", P.le A. Moro 5, 00185 Rome, Italy

Received May 22, 2007. In Final Form: July 11, 2007

Energy dispersive X-ray diffraction was applied to investigate the role of the spacer stereochemistry on the structure of the solid supported aggregates of three stereoisomeric cationic gemini surfactants, 2,3-dimethoxy-1,4-bis-(*N*-hexadecyl-*N,N*-dimethylammonio)butane dibromide. Solid-supported Gemini surfactant aggregates self-assemble into highly interdigitated multilayer stacks. Structural properties, such as the bilayer thickness, the headgroup size, the thickness of the hydrophobic core, and the size of the interbilayer water region, were derived from electron density profiles. Results show that the stereochemistry of the spacer controls the structural properties of the solid-supported interfacial aggregates.

Introduction

Gemini surfactants are a wide class of amphiphilic molecules possessing two hydrophobic tails and two hydrophilic headgroups connected by a spacer of various kind.¹

Geminis are currently used in industrial detergency and have shown efficiency in skin care, antibacterial property, metal-encapped porphyrine, vesicle formation, construction of high-porosity materials, etc. Furthermore, it has recently been shown that this kind of molecule can display higher transfection activities as compared with traditional cationic surfactants.

It is well recognized that satisfactory progresses in transfection efficiency require a full understanding of the roles played by all of the physical-chemical properties of surfactants.² Among these, stereochemistry is known to play a major role in the physico-chemical features of molecular aggregates.³ In fact, stereochemistry of amphiphiles has been reported to have a role in the morphology^{3a} and in the stability^{3b} of aggregates; it influences the transition temperature of liposome bilayers^{3c} and governs the fission and/or fusion processes induced by calcium ions.^{3d} At the aggregate level, the consequences of different stereochemical information at the molecular level are extremely important considering that these systems are investigated as model systems of biological membranes or as drug carriers. Upon aggregation, the information codified in the monomers is translated to the aggregate through recognition processes, and it governs the morphology and the physicochemical features of the aggregate. The stereochemistry of the stereogenic centers on the spacer controls the water exposure of hydrophilic groups and consequently the tendency to assemble, the chain packing, the interface curvature, and the morphology of the aggregate. Even though previous investigations have dealt with the influence of stereo-

chemistry on the physicochemical features of molecular aggregates,³ little if any has been reported on the effect of stereochemistry on the structure of solid-supported aggregates. Knowledge of interfacial aggregation not only complements our understanding of solution aggregation behavior but also has relevance for device applications involving surfactant-templated thin films and membranes.⁴ For the purpose of investigating structure, there are several advantages to studying solid-supported oriented samples. In particular, aligned samples are excellent model systems of biological membranes and allow for more accurate diffraction analyses and, in turn, for more detailed structural information.⁵

Some of us have recently reported on the effect of the stereogenic centers on the aggregation behavior of the diastereomeric gemini in water.⁶

To extend that research, we have investigated the role of the spacer stereochemistry on the structural properties of the solid-supported self-assembled aggregates in the biologically relevant full hydration condition.

Here we report an energy dispersive X-ray diffraction (EDXD) study of the stereoisomers of the cationic gemini surfactant **1** (Figure 1), i.e., (2*S*,3*S*)-2,3-dimethoxy-1,4-bis(*N*-hexadecyl-*N,N*-dimethylammonium)butane dibromide, **1a**, (2*R*,3*R*)-2,3-dimethoxy-1,4-bis(*N*-hexadecyl-*N,N*-dimethylammonium)butane dibromide, **1b**, and (2*S*,3*R*)-2,3-dimethoxy-1,4-bis(*N*-hexadecyl-*N,N*-dimethylammonium)butane dibromide, **1c**.

Materials and Methods

Samples Preparation. Surfactants **1** were prepared and purified as previously described.⁶

A 0.012 M aqueous solution of **1** was prepared by adding 1 mL of bidistilled water to 10 mg of surfactant **1** and gently heating until completely dissolved. Oriented samples were prepared by spreading a few drops of the lipid solution onto the oriented surface of cleaned silicon wafers. After evaporation of the solvent, the samples were kept under vacuum for 12 h to remove any traces of solvent. The

* Author to whom correspondence should be addressed. E-mail: r.caminiti@caspur.it. Tel: +39 06 49913661. Fax: +39 06 490631.

[†] Department of Chemistry.

[‡] IMC-CNR c/o Department of Chemistry.

(1) Luchetti, L.; Mancini, G. *Langmuir* **2000**, *16*, 161.

(2) Safinya, C. R. *Curr. Opin. Struct. Biol.* **2001**, *11*, 440.

(3) (a) Furchop, J.-H.; Helfrich, W. *Chem. Rev.* **1993**, *93*, 1565. (b) Morigaki, K.; Dallavalle, S.; Walde, P.; Colonna, S.; Luisi, P. L. *J. Am. Chem. Soc.* **1997**, *119*, 292. (c) Jaeger, D. A.; Kubicz-Loring, E.; Price, R. C.; Nakagawa, H. *Langmuir* **1996**, *12*, 5803. (d) Sommerdijk, N. A. J. M.; Hoeks, T. H. L.; Synak, M.; Feiters, M.; Nolte, R. J. M.; Zwanenburg, B. J. *Am. Chem. Soc.* **1997**, *119*, 4338.

(4) Manne, S.; Schäffer, T. E.; Huo, Q.; Hansma, P. K.; Morse, D. E.; Stucky, G. D.; Aksay, I. A. *Langmuir* **1997**, *13*, 6382.

(5) Kucerka, N.; Perc, J.; Sachs, J. N.; Nagle, J. F.; Katsaras, J. *Langmuir* **2007**, *23*, 1292.

(6) Bello, C.; Bombelli, C.; Borocci, S.; Di Profio, P.; Mancini, G. *Langmuir* **2006**, *22*, 9333.

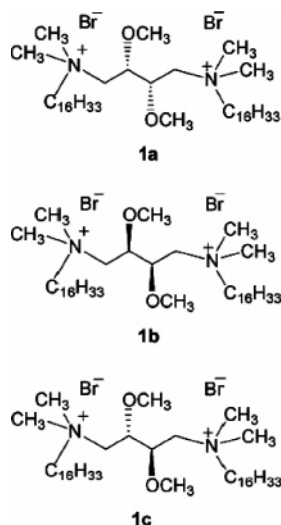


Figure 1. Structure of the studied cationic gemini surfactants: **1a**–**1c**.

lipid films were fully hydrated from a water-saturated atmosphere using a hydration chamber designed to overcome the experimental inadequacy that had previously led to the vapor pressure paradox.⁷ The hydration chamber used is elsewhere described in detail.⁸ It allows achieving full hydration, minimization of temperature gradients, having a water's effective evaporation area and a "vapor volume" suitable to perform both structural and kinetic studies by EDXD.

EDXD Experiments. X-ray diffraction experiments were carried out by using an EDXD apparatus described elsewhere.⁹ An incident polychromatic X-ray radiation was used, and the diffracted beam was energy resolved by a solid-state detector located at a suitable scattering angle θ . The diffractometer operates in vertical θ/θ geometry and is equipped with an X-ray generator (W target), a collimating system, step motors, and a solid-state detector connected via an electronic chain to a multichannel analyzer. The X-ray source is a standard Seifert tube operating at 50 kV and 40 mA, using Bremsstrahlung radiation, and the detecting system is composed of an EG&G liquid nitrogen cooled ultrapure Ge solid-state detector connected to a PC through ADCAM hardware. Both the X-ray tube and the detector can rotate around a common center where the sample is placed. The diffracted intensity was normalized to the incident polychromatic radiation and to all the parasitic effects. Background scattering from the substrates was subtracted. The uncertainty associated with θ is $\Delta\theta = 0.001^\circ$, and it directly affects the uncertainty Δq associated with the transfer momentum q ($q = \alpha E \sin \theta$, $\alpha = 1.01354 \text{ \AA}^{-1} \text{ keV}^{-1}$). Typical acquisition times were 1000 s. Biological samples are not damaged by EDXD experiments as elsewhere discussed.¹⁰

Data Analysis. Due to the bilayer nature of lipid membranes, the electron density profile (EDP) has a center of symmetry in the middle of the bilayer. The electron density profile, $\Delta\rho$, along the normal to the bilayers, z , was then calculated as a Fourier sum of cosine terms^{11,12}

$$\Delta\rho = \frac{\rho(z) - \langle\rho\rangle}{[\langle\rho^2(z)\rangle - \langle\rho\rangle^2]^{1/2}} = \sum_{l=1}^N F_l \cos\left(\frac{2\pi lz}{d}\right) \quad (1)$$

where $\rho(z)$ is the electron density, $\langle\rho\rangle$ its average value, N is the highest order of the fundamental reflection observed in the XRD pattern, F_l is the form factor for the $(00l)$ reflection, d is the thickness

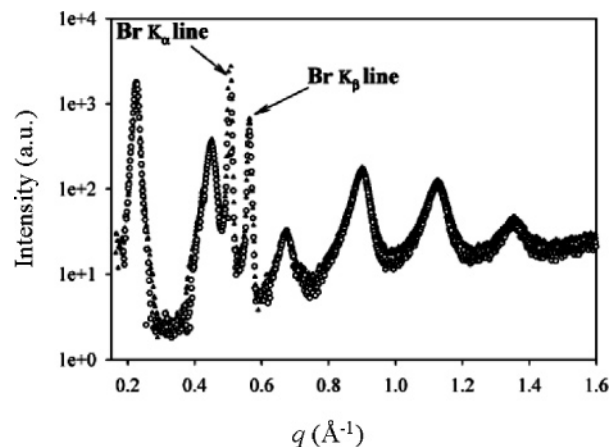


Figure 2. EDXD patterns of **1a** (open circles) and **1b** (black triangles). The Br–K fluorescence lines are superimposed on the pure diffraction pattern and indicated by arrows. To clarity, the intensity of **1b** was divided by 1.05 in order to better discriminate the EDXD patterns.

of the repeating unit including one lipid bilayer and one water layer. Each form factor F_l was calculated from the integrated intensity $I_l = F_l^2/C_l$ under the l th diffraction peak, where C_l is the Lorentz-polarization correction factor for oriented samples. The previous equation determines the form factors except for the phase factor which must be ± 1 for symmetric bilayers. The phase problem, i.e., the choice of the best sign sequence for the structure factor, was solved as previously proposed.^{11,12} The sign combination used to calculate the electron density profile is $(- - + - + +)$ relative to the structures factors F_1, F_2, F_3, F_4, F_5 , and F_6 .

Results and Discussion

Figure 2 shows the EDXD patterns of fully hydrated **1a** and **1b** samples. In the patterns, six $(00l)$ Bragg reflections are observed arising from a multilamellar structure with periodicity $d = 2\pi/q_{001} = 27.9 \text{ \AA}$.¹³ As expected, **1a** and **1b** exhibit the same structural features.

Given the molecular structure of **1** samples (C_{16} alkyl chains plus a polar headgroup), the observation of an extremely small lamellar periodicity, d , could be due to the formation of interdigitated multibilayers with a high degree of interpenetration of alkyl chains.

A deeper sight into the diffraction data allows us to recognize the presence of disorder in the multibilayers system. Indeed, we observe that the intensity of Bragg reflections decreases with the order of diffraction. In addition, the decrease in intensity is also accompanied by a progressive broadening of Bragg peaks proportional to the diffraction order l . Looking at the X-ray patterns of Figure 2, we also observe the presence of diffuse scattering between Bragg reflections. Although diffraction peaks represent interbilayer spatial coherence,¹⁴ diffuse scattering arises from diffraction lacking such a coherence and represents multibilayer-incoherent diffraction.¹⁵ It is relevant to observe that such a scattering curve between peaks becomes higher the farther from the origin.

These observations allow us to identify the disorder of the **1a** multibilayer system as stacking order disorder.¹⁵ This kind of

(11) Luzzati, V.; Mariani, P.; Delacroix, H. *Makromol. Chem., Macromol. Symp.* **1998**, *15*, 1.

(12) Francescangeli, O.; Rinaldi, D.; Laus, M.; Galli, G.; Gallot, B. *J. Phys. II France* **1996**, *6*, 77.

(13) Caracciolo, G.; Mancini, G.; Bombelli, C.; Luciani, P.; Caminiti, R. *J. Phys. Chem. B* **2003**, *107*, 12268.

(14) Pabst, G.; Koschuch, R.; Pozo-Navas, B.; Rappolt, M.; Lohner, K.; Lagner, P. *J. Appl. Cryst.* **2003**, *36*, 1378.

(15) Blaurock, A. E. *Biochim. Biophys. Acta* **1982**, *650*, 167.

(7) Katsaras, J. *Biophys. J.* **1998**, *75*, 2157.

(8) Caracciolo, G.; Petrucci, M.; Caminiti, R. *Chem. Phys. Lett.* **2005**, *414*, 456.

(9) Caminiti, R.; Rossi Alberini, V. *Int. Rev. Phys. Chem.* **1999**, *18*, 2.

(10) Caracciolo, G.; Amiconi, G.; Bencivenni, L.; Boumis, G.; Caminiti, R.; Finocchiaro, E.; Maras, P.; Paolinelli, C.; Congiu Castellano, A. *Eur. Biophys. J.* **2001**, *30*, 163.

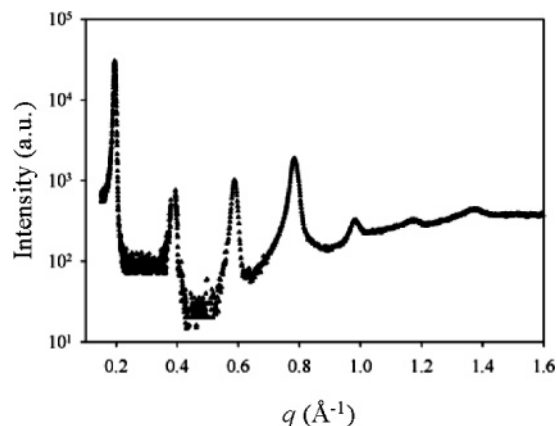


Figure 3. EDXD pattern of **1c**.

disorder, usually referred to as “second-order disorder”,¹⁵ accounts for the presence of small variations in the bilayers separation and is described within the paracrystalline theory.¹⁵ As the position of an individual fluctuating layer in a paracrystal is determined only by its nearest neighbor membranes, the crystalline long-range order is lost. However, Bragg-peak scattering is still observed (the Bragg peaks of Figure 2) and is due to the fact that there is quasi-long-range order normal to the membrane plane.

Figure 3 shows the EDXD pattern of the fully hydrated **1c** sample. In the X-ray pattern, seven orders of diffraction are observed. From the position of the first-order Bragg peak, we could calculate the lamellar periodicity $d = 31.9$ Å. The X-ray pattern of Figure 3 exhibits the same general features of those reported in Figure 2. This means that also the **1c** multibilayers stack is affected by “second-order disorder”.¹⁵ However, the meso form, **1c**, presents a larger value in d -spacing of about 4 Å compared to that obtained for both **1a** and **1b** samples. Indeed, the different stereochemistry imposes different orientations of the methoxy groups⁶ determining different intermolecular interactions and different packings of monomers inside the aggregates as well as a different degree of hydration of the polar headgroups. In brief, the stereochemistry of the headgroup influences the structural properties of solid-supported aggregates formed by stereoisomeric geminis **1**.

To elucidate this point, we calculated EDPs by which detailed structural information, such as the size of the headgroup and the thickness of the hydrocarbon core (HC), can be retrieved.¹⁴

Figure 4 shows the EDPs of **1a** (top panel) and **1c** (bottom panel). The EDPs of Figure 4 exhibit two strong maxima (marked by asterisks) corresponding to the electron-dense surfactant headgroups (where Br counterions are located). One common feature of these profiles is the absence of a trough in the center of the hydrocarbon region, which corresponds to the usual location of the CH₃ groups in the middle of the bilayer.^{14,15} In noninterdigitated lamellar phases, the electron-dense headgroups are usually represented by two Gaussians and the electron-sparse region at the methyl terminus of the hydrocarbon chains by another Gaussian with negative amplitude.¹⁵ As evident, this is not the case of the EDPs of Figure 4. In contrast, the two pronounced minima in the EDPs (marked by black circles) indicate that the CH₃ groups are not positioned in the middle of the bilayer but are close to the polar headgroups. The two density troughs, separated by about 13 and 16 Å for **1a** and **1c**, respectively, suggest that the surfactant chains from opposing monolayers have interpenetrated.¹⁶ The central minimum (marked by a black

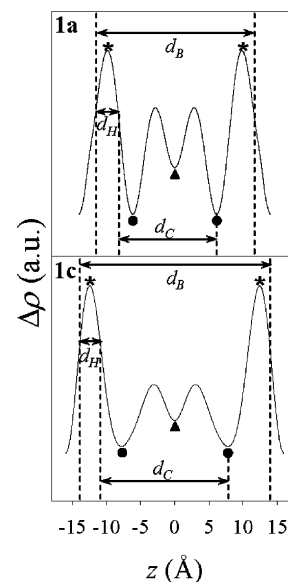


Figure 4. Electron density profiles along the normal to the bilayers of **1a** and **1c**. The full width at half-maximum of the Gaussians representing the polar headgroups (marked by asterisks) is a good estimate of the headgroup size.¹⁴ The two density troughs (marked by black circles) are due to the terminal CH₃ groups and suggest that the surfactant chains from opposing monolayers have interpenetrated.¹⁶ The central minimum (marked by a black triangle) corresponds to the interdigitated region where the methylene groups are located. Structural parameters are shown.

triangle) corresponds to the interdigitated region where the methylene groups are located.¹⁷

The presence of the spacer induces a separation of the chains larger than in single-head surfactants. This would potentially cause voids between chains in the bilayer interior.¹⁶ Since the energy of formation of holes in hydrocarbons is extremely large,¹⁷ the chains tend to interpenetrate to eliminate the voids. The resulting interdigitated structure is the lowest energy phase.¹⁶

Although d can be determined from diffraction patterns with high accuracy by the Bragg’s law, it is sometimes difficult to split d into the membrane components:¹⁵ the bilayer thickness, d_B , and the water layer thickness, d_W . One conventional way to determine the structural parameters, known as the Luzzati method,¹⁸ is by $d_B = \phi_L d$, where ϕ_L is the lipid volume fraction. However, this method does not account for water penetrating into the bilayer region and has been questioned on several occasions.¹⁴

More recent methods¹⁹ retrieve the principal structural parameters directly from the electron density profile. These methods usually define d_B as the maximal thickness occupied by surfactants thereby including water molecules associated with the hydration shell of the polar headgroups.^{15,19} According to such a definition,^{19,20} the bilayer thickness is therefore given by $d_B = d_{HH} + d_H$ where d_{HH} is the distance between the strong maxima in EDP and d_H is the headgroup size.

Due to the possible low resolution of the EDP, the definition of the boundary between the membrane and the interbilayer water region is often not trivial¹⁵ and, consequently, the calculation of d_H can be difficult. However, this is not the case for our EDXD measurements. Indeed, the high number of Bragg reflections observed allowed us to obtain high-resolution EDPs (Figure 4).

(17) Israelachvili, I.; Marcelja, S.; Horn, R. G. *Q. Rev. Biophys.* **1980**, *13*, 121.

(18) Luzzati, V.; Husson, F. *J. Cell Biol.* **1962**, *12*, 207.

(19) Pabst, G.; Rappolt, M.; Amenitsch, H.; Laggner, P. *Phys. Rev. E* **2000**, *62*, 4000.

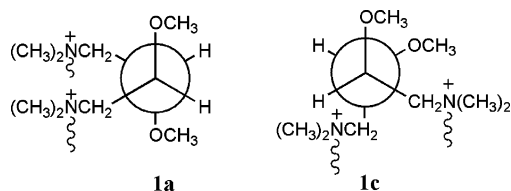
(20) Caracciolo, G.; Pozzi, D.; Caminiti, R. *Appl. Phys. Lett.* **2007**, *90*, 183901.

(16) McIntosh, T. J.; McDaniel, R. V.; Simon, S. A. *Biochim. Biophys. Acta* **1983**, *731*, 109.

Table 1. Structural Parameters of **1a and **1c** as Obtained by EDPs Profiles^a**

	1a	1c
d (Å)	27.9	31.9
d_B (Å)	25.6	28.2
d_W (Å)	2.3	3.7
d_H (Å)	4.3	3.3
d_C (Å)	15.3	18.7

^a d is the lamellar periodicity, d_B is the bilayer thickness, d_W is the water layer thickness, d_H is the headgroup size, and d_C is the hydrocarbon chain length.

**Figure 5.** Newman projection of **1a** and **1c**.

As recently suggested by Pabst et al.,¹⁹ d_H , that is absolutely needed to calculate d_B , can be estimated from the full width at half-maximum of the Gaussian representing the headgroup (Figure 4). As a result, the HC thickness, d_C , and the thickness of the interbilayer water region, d_W , can be retrieved by simple geometric calculations as illustrated in Figure 4. The values of d , d_B , d_W , d_H , and d_C obtained for **1a** and **1c** samples are shown in Table 1.

We observe that the headgroup size of **1a** ($d_H = 4.3$ Å) is larger than that of **1c** ($d_H = 3.3$ Å). Such a finding is in good agreement with the molecular models of **1a** and **1c** that have been recently obtained by molecular modeling⁶ and illustrated in Figure 5 as Newman projections. Indeed, it has been shown that in **1c** both methoxy groups are exposed to the aqueous solvent while, in **1a**, only one of the methoxy groups is exposed to water and the other is oriented toward the hydrophobic region of the alkyl chains (see Newman projections of Figure 5). Remembering that EDP is a 1D representation of the bilayer structure, the different orientation of the methoxy groups may therefore explain the difference in the headgroup size observed by EDXD experiments.

The thickness of the hydrophobic region of **1c** ($d_C = 18.7$ Å) is larger than that of **1a** ($d_C = 15.3$ Å). In principle, the observed difference could be due to a more folded configuration of the alkyl chains of **1a** and/or to a higher degree of interpenetration of alkyl chains.

The 1D space (normal to the membrane plane) occupied by one single surfactant molecule can be estimated by $d_1 = d_C + d_H$. Such a value, that is larger in the case of **1c** ($d_1 = 22$ Å) with respect to **1a** ($d_1 = 19.6$ Å), can be used to estimate the degree of interdigitation, X_i , of the leaflets by the simple geometric relation, $X_i = (2d_1 - d_B)/d_B$. By using the structural parameters

listed in Table 1, we obtain $X_i = 0.53$ and 0.56 for **1a** and **1c**, respectively. This finding indicates that, within experimental errors, the interpenetration of the alkyl chains is almost the same for **1a** and **1c**, respectively. Thus, we conclude that the smaller size of **1a** molecules within self-assembled aggregates can be entirely ascribed to the more folded configuration of the alkyl chains. Also this result is in very good agreement with the configuration of the acyl chains of **1a** monomers.⁶ The more folded configuration of the hydrophobic tails of **1a**, as revealed by X-ray analysis, is due to the headgroup orientation with respect to acyl chains. Indeed, it is well recognized that the headgroup conformation and its orientation with respect to the hydrophobic tails control the packing properties of the self-assembled aggregates.²¹ Recently, diastereomeric surfactants have been found to show a different degree of chain order resulting in more folded configuration of the chains.²²

Last, the thickness of the interbilayer water region was found to be larger in the case of **1c** ($d_W = 3.7$ Å) with respect to **1a** ($d_W = 2.3$ Å). It is well-known that the headgroup conformation controls the packing of monomers in the aggregates¹³ and that such a molecular packing is a major factor in modulating membrane structure. In particular, headgroup orientation affects the properties of the interfacial region, a site of complex interactions between headgroups and water molecules.^{23,24} Recent studies have also shown that the number of water molecules held around the different components of the headgroup strictly depends on the directional hydrogen bonding ability in the headgroup²⁵ and that such an ability is strongly coupled to headgroup orientation. Thus, we believe that the completely different orientation of the methoxy groups⁶ can also account for the different thickness of the water region.

Conclusions

In summary, we have investigated the role of the stereochemistry of the spacer on the structure of the interfacial aggregates of **1** Gemini surfactants. We have shown that **1** Gemini surfactants self-assemble into multibilayer systems with highly interdigitated alkyl chains. Our structural findings underline the crucial role of the stereochemistry of the spacer on the structural properties of solid-supported **1** multibilayers, such as the bilayer thickness, the headgroup size, the thickness of the hydrophobic core and the size of the interbilayer water region.

LA7014995

(21) (a) Tickle, D.; Gorge, A.; Jennings, K.; Camilleri, P.; Kirby, A. J. *J. Chem. Soc. Perkin Trans.* **1998**, *2*, 467. (b) van Buuren, A. R.; Berendsen, H. J. C. *Langmuir* **1994**, *10*, 1703.

(22) Borocci, S.; Ceccacci, F.; Galantini, L.; Mancini, G.; Monti, D.; Scipioni, A.; Venanzi, M. *Chirality* **2003**, *15*, 441.

(23) Binder, H.; Gutberlet, T.; Anikin, A.; Klose, G. *Biophys. J.* **1998**, *74*, 1908.

(24) Binder, H.; Gawrisch, K. *Biophys. J.* **2001**, *81*, 969.

(25) Jay Mashl, R.; Larry Scott, H.; Subramaniam, S.; Jakobsson, E. *Biophys. J.* **2001**, *81*, 3005.